JOURNAL OF SEMICONDUCTOR TECHNOLOGY AND SCIENCE, VOL.18, NO.3, JUNE, 2018
https://doi.org/10.5573/JSTS.2018.18.3.328
ISSN(Print) 1598-1657
ISSN(Online) 2233-4866

# MATLAB/Simulink Pulse-echo Ultrasound System Simulator with Electrical Impedance Matching

**Sangmin Shin, Taehoon Kim, and Suhwan Kim**

***Abstract*—In an ultrasound system, impedance matching between a transducer and an electronics is one of the crucial factors to determine the performance. An electronics must operate with different transducers, which have their characteristic impulse responses and widely varying impedances so that impedance matching is difficult. Also, the parasitic element is another factor that impedes the impedance matching. In this paper, using MATLAB and Simulink, we simulate a pulse-echo ultrasound system and the matching network which is required to allow the use of transducers with widely differing impedances. Our simulation includes models of the high-voltage transmitter, the transmission interface, the acoustic subsystem which includes wave propagation and reflection, the receiving interface, and the front-end receiver, as well as a lumped model of the matching interface which can easily be adjusted by the designer. The simulated pulse-echo behavior was in close agreement with experimental measurements.**

***Index Terms*—Ultrasound imaging system, behavioral modeling, ultrasonic transducers, parasitic elements, impedance matching, MATLAB/Simulink**

Manuscript received Aug. 7, 2017; accepted Mar. 4, 2018
Department of Electrical and Computer Engineering and the Inter-University Semiconductor Research Center (ISRC), Seoul National University, Seoul, 08826, Korea
E-mail : suhwan@snu.ac.kr

## I. INTRODUCTION

Ultrasound medical imaging is a largely non-invasive way of obtaining immediate displays of body tissues which are widely used for diagnosis in fields such as obstetrics, gynecology, orthopedics, and oncology. Ultrasound systems can be used with a wide range of transducers, allowing many different organs to be scanned, but different transducers can have very different values of impedances and impulse response.

Coping with the impedance mismatches is a major issue in the design of ultrasound systems for use with a range of transducers, as their impedances can range from less than 50 Ω to 10 kΩ [1, 2]. The parasitic elements and on-resistances in the receiver's input path impede the impedance matching between a transducer and a front-end receiver, which will change the amplitude of the received echoes [3, 4].

Another design challenge is the requirement for the high-voltage transmitter to generate pulses of different shapes to suit the impulse response of the transducer. The two-way impulse response of a transducer also determines the parameters of the components in the front-end receiver, such as the gains and bandwidths of amplifiers, the sampling-rate, and the resolution of the analog-to-digital converter (ADC).

There have been many efforts to simulate the behavior of an ultrasound system on a computer, mostly focused on the transducer. Theoretical models, such as these developed by Mason [5], Redwood [6], Krimholtz, Leedom and Matthaei (KLM) [7], and Leach [8], which is based on material properties and physical dimensions, are commonly used for optimizing the design of a transducer. But when the transducer is already available,

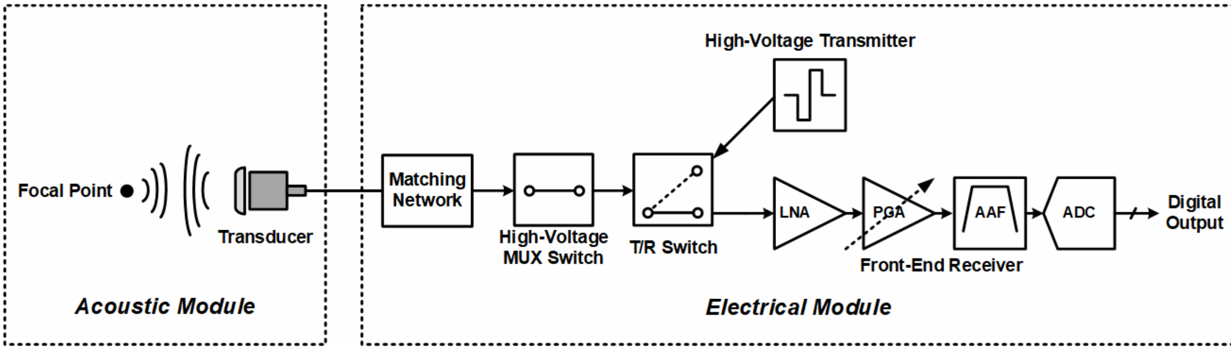


**Fig. 1.** Block diagram of an ultrasound system.

an analytical model can be constructed from experimental measurement [9]. From the theoretical and analytical models, the pulse-echo responses can be investigated. The electrical characteristics of an ultrasonic transducer are often abstracted using the Butterworth-Van Dyke (BVD) model [10], which has been enhanced to broadband [11]. In the BVD model, a transducer is represented by lumped circuits. This model allows us to simulate the response between a transducer and a load impedance, and the resulting simulation can be used in designing an impedance matching network.

Recently, we proposed an ultrasound system simulator [12] in which both the transducer and the electronics of a pulse-echo ultrasound system are represented in a single MATLAB/Simulink model, which can be used to investigate the pulse-echo responses and analyze the impedance mismatches. In this simulator, both pulse-echo responses and the impedances of the transducer and electronics are represented in MATLAB as transfer functions constructed from measurements. The high-voltage transmitter and the front-end receiver are modeled in Simulink so that they can be optimized by changing the appropriate parameters. Results obtained from this simulation were checked against experimental data obtained from a commercial ultrasound system, ECUBE7, from Alpinion Medical Systems. However, there are some inconveniences in this simulator. The impedances have to be measured whenever an electronic component is changed; and the impedances of the transducers and the electronics are not represented as a lumped-component model, so whenever testing the matching network in the simulation require the matching network to be constructed by soldering on the hardware so that the impedance can be measured.

We have now developed a new simulator that pulse-echo transient simulation is available with including an optimized impedance matching network. In this simulator, the input impedance of the front-end receiver is modeled using equivalent circuits, making it easy to modify and to assess its effectiveness. Since, the input impedance of the front-end receiver is modeled as lumped model, impedance matching network design and the effectiveness test is also available in the proposed simulator. An impedance matching network can be designed using the Smith chart and the matching network circuits are then incorporated into the impedance model of the front-end receiver. Then, its pulse-echo response can be simulated. The accuracy of the simulator has been verified by comparing simulation results with measured data [12].

The rest of this paper is organized as follows: Section II is an overview of our pulse-echo ultrasound system simulator. In Section III, the design of the front-end receiver's input impedance, the design of the matching network, and the simulation of pulse-echo behavior are presented. In Section IV, we show here we checked the simulation results against measured data. We draw conclusion in Section V.

## II. Overview of The Proposed Simulator

Fig. 1 is a block diagram of the ECUBE7 ultrasound system, which consists of a high-voltage transmitter, a transducer, a matching network, a high-voltage multiplexer (MUX) switch, a transmit/receive (T/R) switch, and a front-end receiver. The high-voltage transmitter generates a high-voltage pulse and applies it into the transducer, which converts it into an acoustic pulse, which is directed towards a focal point. The transducer converts the reflected acoustic echo signal

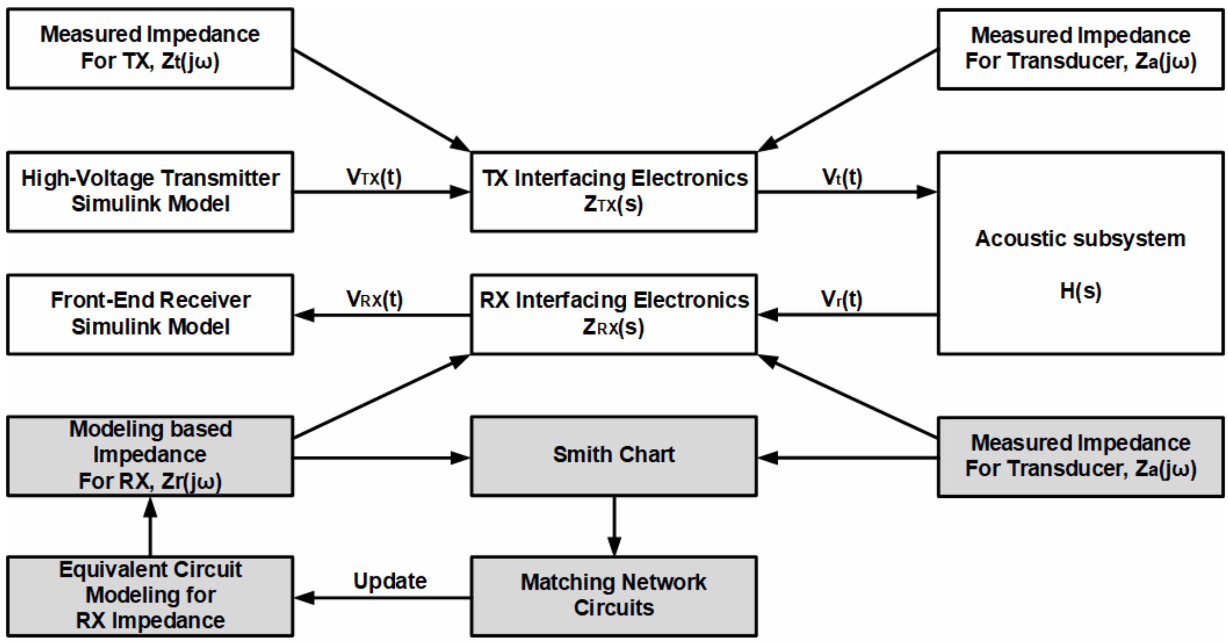


**Fig. 2.** The proposed pulse-echo ultrasound system simulator.

into an electrical echo signal, which passes through the high-voltage MUX switch, the T/R switch, and the front-end receiver. The high-voltage MUX switch selects the channel and the T/R switch cycles between transmit and receive mode. The front-end receiver, which consists of a low-noise amplifier (LNA), a programmable-gain amplifier (PGA), an anti-aliasing filter (AAF), and an ADC which amplifies and digitizes electrical echo signal, is connected to the transducer through an impedance matching network.

Fig. 2 is a block diagram of our proposed pulse-echo ultrasound system simulator, which is constructed by using the same methodology as our previous simulator [12]. The white blocks represent the pulse-echo ultrasound system behavior and the gray blocks represent the impedance matching optimization process in the proposed modeling. In Fig. 2, the circuits of the high-voltage transmitter and the front-end receiver are modeled with Simulink and the pulse-echo behavior from output of high-voltage transmitter to input of front-end receiver is modeled based on measurements. The model of the acoustic sub-system is based on the electro-acoustic transfer function $H(s)$, which represents the way in which an outgoing electrical pulse $V_t(t)$ is transformed into an incoming electrical echo signal $V_r(t)$. This process includes electro-acoustic conversion of the transmitted pulse, acoustic propagation, reflection, and acoustic-electrical conversion of the echo signal. We build $H(s)$ by measuring values of $V_t(j2\pi f_k)$ and $V_r(j2\pi f_k)$, and is then computed by MATLAB's *rationalfit* function. On the other hand, the transmitter interfacing electronics $Z_{TX}(s)$ and the receiver interfacing electronics $Z_{RX}(s)$ are required for the voltage division by the impedances. In transmit mode, the electrical pulse, $V_{TX}(t)$ from the high-voltage transmitter needs to be multiplied by $Z_a/(Z_t+Z_a)$; and in receive mode, the electrical echo signal $V_r(t)$ needs to be multiplied by $Z_r/(Z_a+Z_r)$, where $Z_t$, $Z_a$, and $Z_r$ are respectively the impedances of the high-voltage transmitter, the transducer, and the front-end receiver. $Z_t$ reflects the impedance of the high-voltage transmitter, T/R switch, and high-voltage MUX switch. Also, $Z_r$ reflects the impedance of the LNA, T/R switch, and high-voltage MUX switch. When the impedances $Z_a(j2\pi f_k)$, $Z_t(j2\pi f_k)$, and $Z_r(j2\pi f_k)$ have been measured, the transfer functions $Z_{TX}(s)$ and $Z_{RX}(s)$ can able be determined using *rationalfit* function. The transfer function from the transmitted pulse $V_{TX}(t)$ to the received echo signal $V_{RX}(t)$ can be written as follows:

$$\frac{V_{RX}(s)}{V_{TX}(s)} = Z_{TX}(s)H(s)Z_{RX}(s) = \frac{Z_a}{Z_t+Z_a}(s)H(s)\frac{Z_r}{Z_a+Z_r}(s), \quad (1)$$

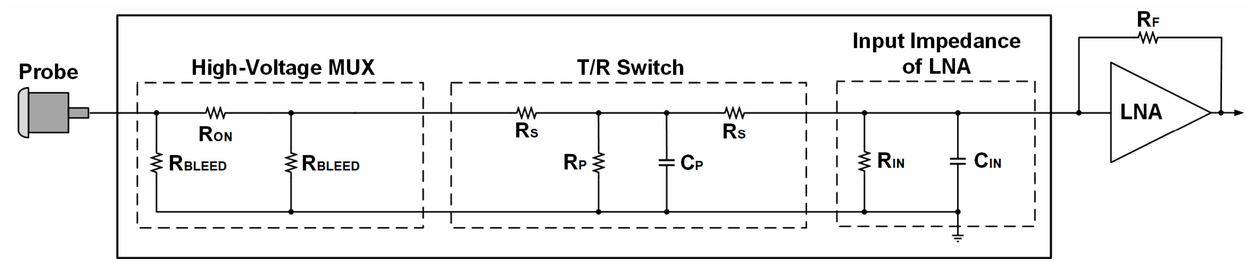


**Fig. 3.** Equivalent circuit of the input impedance of the front-end receiver.

where $V_{TX}(s)$ and $V_{RX}(s)$ are the Laplace transforms of $V_{TX}(t)$ and $V_{RX}(t)$, respectively. Together with the Simulink models of the high-voltage transmitter and the front-end receiver, the function $V_{RX}(s)/V_{TX}(s)$ constitutes a model of the overall behavior of a pulse-echo ultrasound system.

The impedance of the front-end receiver $Z_r(j2\pi f_k)$, is based on the equivalent circuit modeling to build receiver interfacing electronics $Z_{RX}(s)$. The equivalent circuit modeling for the front-end receiver's input impedance gives us two advantages in terms of a simulation. For the perspective of electronics' designer, the impedance matching between a transducer and a front-end receiver is troublesomeness because the amplitude of the echo signal from the transducer to front-end receiver is significantly small and it requires the matching network to be inserted between the transducer and the front-end receiver. Firstly, once the impedances of the high-voltage transmitter, the transducer, and the electro-acoustic transfer function $H(s)$ have been measured, the input impedance of the front-end receiver can easily be modified by adding or removing R, L, C components from the equivalent circuit model if the components of the electronics are changed. In addition, if $Z_r(j2\pi f_k)$ is found from an equivalent circuit model, we can easily combine it with a matching network to build a new $Z_r(j2\pi f_k)$. Then, we can simulate the pulse-echo behavior with observing the effects of the matching network in the proposed simulator.

## III. MODELING

### 1. Receiver Input Impedance Modeling

Fig. 3 shows the equivalent circuit model of the input impedance of the front-end receiver. In the ECUBE7 ultrasound system, the high-voltage MUX chip and the T/R switch chip are in front of the LNA, and therefore we need to consider the impedances of these two chips as well as that of the LNA [13]. The appropriate parameters can be obtained from chip datasheets. The on and bleed resistances of the high-voltage MUX switch must be modeled [14]. The bleed resistor is connected in parallel with the output of a high-voltage power supply to discharge the power supply's filter capacitors when the equipment is turned off. The on-resistance and the parasitic resistance and the capacitance of the T/R switch are also built into an equivalent circuit model [15]. In our model of the ECUBE7, $R_{ON}$ is set to 19 Ω and $R_{BLEED}$ is set to 35 kΩ for the high-voltage MUX; $R_S$ is set to 13/2 Ω, $R_P$ is set to 100 kΩ and $C_P$ is set to 40 pF for the T/R switch; and $R_{IN}$ is set to 40 Ω, $C_{IN}$ is set to 20 pF for the input impedance of the LNA. To determine the input impedance of LNA, we can select either an active termination mode or a non-active termination mode [13]. The non-active termination is used in this paper to determine the parameters of the input impedance of LNA because measurements to validate the simulation are made without active termination. In the non-active termination mode, the value of the feedback resistor $R_F$ is effectively infinite. Accordingly, the input impedance of the front-end receiver $Z_r(s)$ can be derived as follows:

$$Z_{LNA}(s) = \frac{1}{C_{IN}s} \parallel R_{IN}, \tag{2}$$

$$Z_{T/R+LNA}(s) = (((Z_{LNA}(s) + R_P) \parallel \frac{1}{C_P s}) \parallel R_P) + R_S, \tag{3}$$

$$Z_r(s) = ((Z_{T/R+LNA}(s) \parallel R_{BLEED}) + R_{ON}) \parallel R_{BLEED}. \tag{4}$$

By following (4), an equivalent circuit model can be expressed as an s-domain function $Z_r(s)$ in MATLAB, which can then be converted into the impedance function $Z_r(j2\pi f_k)$.

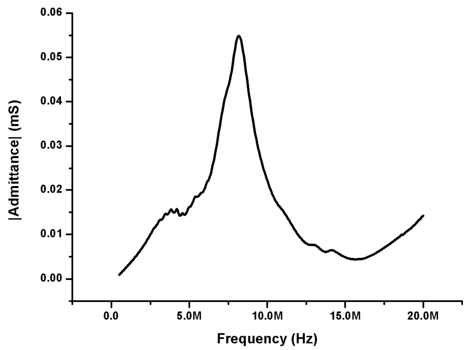


**Fig. 4.** Admittance of the L3-12 transducer.

## 2. Impedance Matching Network

A Smith chart allows us to find the impedance matching network circuit that achieves maximum power transfer. Maximum power is delivered from a source to a load if the load impedance is the complex conjugate of the source impedance. If the load and the source are unmatched, impedance matching network is required to maximize the power transfer from the source to the load. An impedance matching network changes the source impedance to the load impedance point by adding capacitors/inductors in series or parallel. An inductor in parallel moves the impedance point along a curve of constant resistance, while a capacitor in series, which moves the impedance point along a curve of constant conductance.

In our case, the 128-element Alpinion Medical Systems' L3-12 transducer is the source impedance. Fig. 4 shows the measured admittance of this transducer, which has a single resonant frequency at 8 MHz. By considering the large impedance mismatch and the transducer response at the center frequency, the impedance matching network was therefore chosen to maximize the signal transfer. Fig. 5 shows how the Smith chart is used to select two inductors and one capacitor for the impedance matching network shown in Fig. 6. The impedance of the transducer is 42-j48 Ω and the input impedance of the receiver is 72-j0.8 Ω. The values of $L_1$, $L_2$, and $C_1$ are set to 914.9 nH, 26 nH, and 358.4 pF, respectively.

## 3. Pulse-echo Simulation

The equivalent circuit determining the input

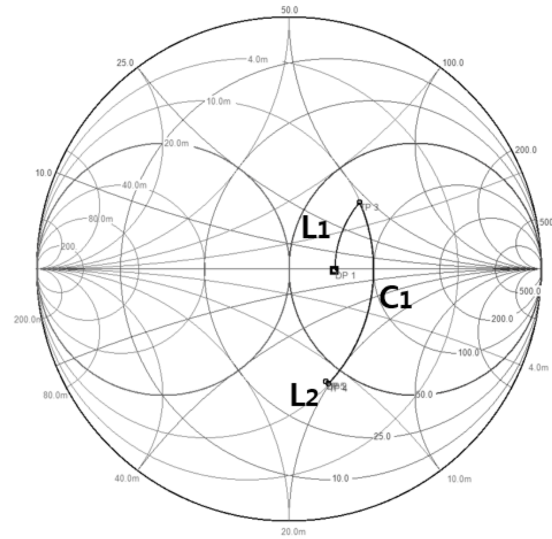


**Fig. 5.** Simith chart for impedance matching network design.

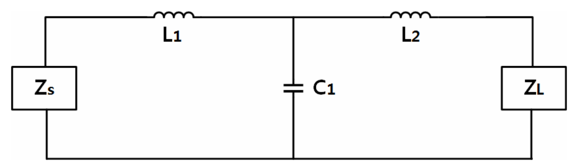


**Fig. 6.** Impedance matching network.

impedance of the receiver can now be modified to incorporate the matching network. If we assume the total impedance of the circuit shown in Fig. 3 as $Z_r(s)$, we can change the impedance of the front-end receiver to $Z_{r,new}(s)$ by introducing appropriate inductances and a capacitance, as follows:

$$Z_{r,new}(s) = L2s + \frac{(Z_r(s) + L1s)(1/C1s)}{(Z_r(s) + L1s) + (1/C1s)}. \qquad (5)$$

We can convert $Z_{r,new}(s)$ to $Z_{r,new}(j2\pi f_k)$ using *bode* and *squeeze* function in MATLAB, and then approximate the transfer function $Z_{RX,new}(j2\pi f_k)$ by using the *rationalfit* function in MATLAB to fit a function of the transfer function to the complex vector data [16, 17]. Finally, we can perform $V_{RX}(s)/V_{TX}(s)$ as mentioned in (1) to simulate pulse-echo behavior. The generation of the high-voltage pulse, amplification of the echo signal, and its digitization are modeled using Simulink and so are the high-voltage MUX switch, the T/R switch, and the matching network circuits. For more detailed discussion of Simulink models, the readers should consult [12].

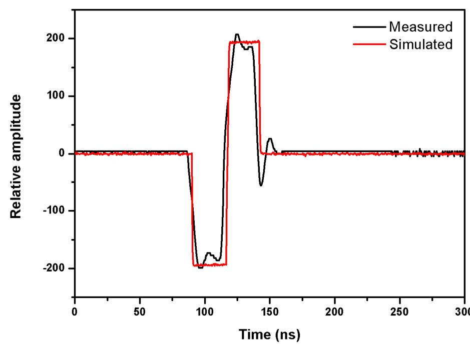


**Fig. 7.** Measured and simulated amplitudes of the high-voltage pulse.

## IV. SIMULATIONS

### 1. Validation and Simulation

The L3-12 transducer was immersed in a water tank, connected to the ECUBE7 ultrasound system by a coaxial cable, and is excited by pulses from the high-voltage transmitter. The transducer produces ultrasound waves which propagate through the water and are reflected by a steel reflector. The transducer converts the returning ultrasound waves to an electrical echo signal, and both outgoing and incoming pulses can be viewed on an oscilloscope. The electrical echo signal goes through amplification, filtering, and analog-to-digital conversion.

Fig. 7 compares the measured waveform of the high-voltage pulse with the waveform from the high-voltage transmitter Simulink model. Fig. 8 compares the measured and simulated echo signals, in both time and frequency domain. For this comparison, the echo signal is measured and simulated between the acoustic subsystem and the front-end receiver. The peak amplitude of the echo signal in Fig. 8(a) is normalized to one, and Fig. 7 and 9(a) show relative amplitudes. Fig. 9 shows both measurements and simulation of the digitized output of the echo signal from the front-end receiver, sampled at 40MSPS. From Fig. 9(b), the difference between the measurement and the simulation results can be expressed as follows:

$$10^{\varepsilon/20} \geq \frac{\sqrt{\sum_{k=1}^{n} | F_0\{f_k\} - F\{f_k\} |^2}}{\sqrt{\sum_{k=1}^{n} | F_0\{f_k\} |^2}}, \qquad (6)$$

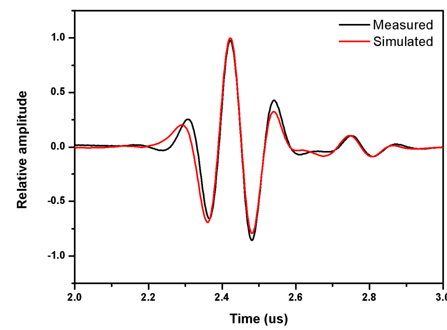


(a)

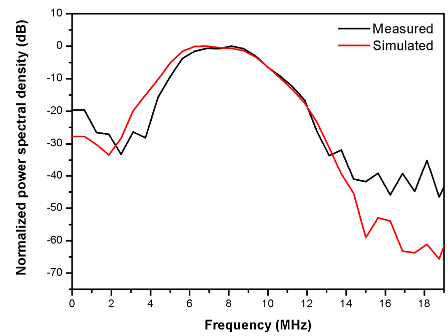


(b)

**Fig. 8.** Measured and simulated amplitude of the echo signal in (a) the time domain, (b) the frequency domain.

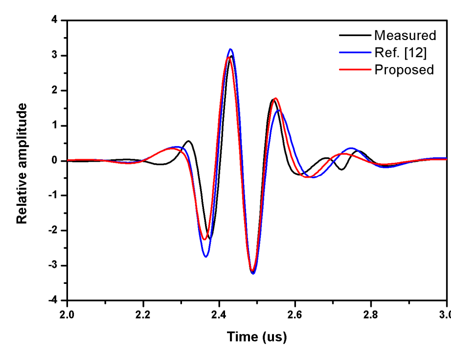


(a)

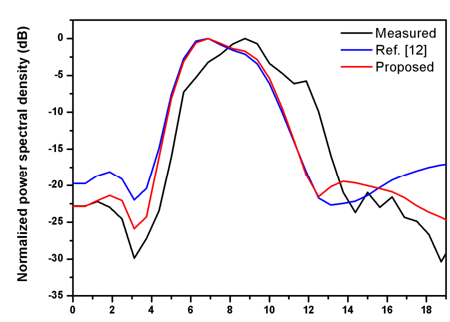


(b)

**Fig. 9.** Digitized output of measurement, result from our previous simulation [12], and from the proposed simulator, in (a) the time domain, (b) the frequency domain.

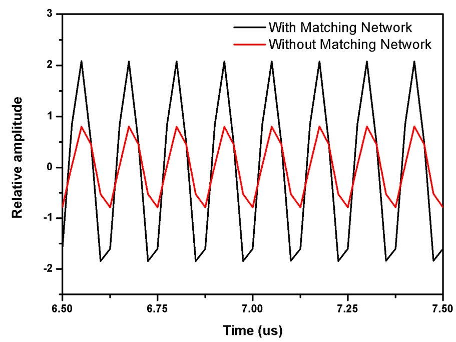


(a)

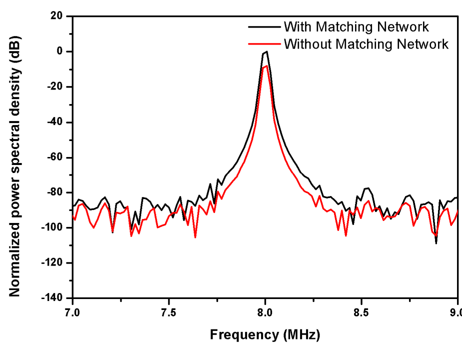


(b)

**Fig. 10.** Output corresponding to an 8 MHz sine input digitized at 40 MSPS in (a) the time domain, (b) the frequency domain.

where ε is the error in dB, $F_0$ is the measured value of $F_0(j2\pi f_k)$ at a frequency $f_k$, and $F$ is the simulation result in the frequency domain. On this basis, the error in our previos simulator [12] is -9.8 dB and the error in the proposed simulator is -12.0 dB. Although, the input impedance of the front-end receiver is modeled using equivalent circuits in the proposed simulator, the simulation result is well-matched with the measurement and our previous simulator [12].

### 2. Testing a Matching Network

One crucial application of our model is the design and test of a matching network, which can be implemented as a parallel compensating inductance, a series compensating inductance, or an 'L' matching network [18]. To observe the effects of a matching network, we simulated the application of an 8 MHz sine wave to the transducer. Fig. 10 shows the digitized output from the model of the combined impedance of the front-end receiver, with and without the matching network, in both the time and frequency domain at a sampling rate of 40 MSPS. The amplitude of the output sine-wave increases when the matching network is included. The narrow-band signal-to-noise ratio (NBSNR) of the digitized output with the matching network is 69.4 dB and without the matching network is 66.7 dB. Where NBSNR is signal power divides by sum of noise power in a 2 MHz band around signal frequency, which is a significant index that directly related to the performance of an ultrasound system [12]. The simulation result shows that the NBSNR is 2.7 dB enhanced because the impedance mismatch is reduced by inserting the electrical matching network in between the transducer and the front-end receiver.

## V. CONCLUSIONS

In this paper, we have presented a simulation of an ultrasound system that models two-way pulse-echo behavior, and allows the effect of an impedance matching network to be observed. This is an improvement on our previous simulator [12] because the input impedance the front-end receiver is modeled as an equivalent circuit. This allows a system designer to observe the pulse-echo behavior produced by different matching circuits simply by changing values of the components in the model, without changing the experimental hardware. Once, the impedance matching network is designed, we can simply add the matching network circuit to the equivalent circuit of the input impedance of the front-end receiver for impedance matched simulation. Results from the simulator show good agreement with the measured data [12] and better influence of the matching network is demonstrated.

## REFERENCES

[1] B. A. J. Angelsen, H. Torp, S. Holm, K. Kristoffersen, and T. A. Whittingham, "Which transducer array is best?" *Eur. J. Ultrasound*, vol. 2, no. 2, pp. 151-164, 1995.

[2] E. Brunner, "Ultrasound system considerations and their impact on front-end components," in *Analog Dialogue.* Analog Devices Inc., 2002, vol. 36, no. 3.

[3] J. Johansson and J. Delsing, "Effects of parasitic electrical components on an ultrasound system: Measurements and simulations using SPICE

models," *Proc. SPIE,* vol. 4946, 2002, pp. 174-182.

[4] J. Johansson, P.-E. Martinsson, and J. Delsing, "Simulation of absolute amplitudes of ultrasound signals using equivalent circuits," *IEEE Trans. Ultrason. Ferroelectr. Freq. Control,* vol. 54, no. 10, pp. 1977-1982, Oct. 2007.

[5] W. P. Mason, *Electromechanical Transducers and Wave Filters*, Van Nostrand, 1948.

[6] M. Redwood, "Transient performance of a piezoelectric transducer," *J. Acoust. Soc. Am.*, vol. 33, no. 4, pp. 527-536, Apr. 1961.

[7] R. Krimholtz, D. A. Leedom, and G. L. Matthaei, "New equivalent circuit for elementary piezoelectric transducers," *Electron. Lett.*, vol. 6, no. 13, pp. 398-399, Jun. 1970.

[8] W. Marshall Leach, Jr., "Controlled-source analogous circuits and SPICE models for piezoelectric transducers," *IEEE Trans. Ultrason. Ferroelect. Freq. Control*, vol. 41, no. 1, pp. 60-66, Jan. 1994.

[9] L. Capineri, L. Masotti, M. Rinieri, and S. Rocchi, "Ultrasonic transducer as a black-box: equivalent circuit synthesis and matching network design," *IEEE Trans. Ultrason. Ferroelect. Freq. Control*, vol. 40, no. 6, pp. 694-703, Nov. 1993.

[10] L. Svilainis, V. Dumbrava, and G. Motiejunas, "Optimization of the ultrasonic excitation state," in *30$^{th}$ Int. Conf. Information Techonology Interfaces*, Dubrovnik, Croatia, Jun. 2008, pp. 791-796.

[11] H. Huang, and D. Paramo. "Broadband electrical impedance matching for piezoelectric ultrasound transducers." *IEEE Trans. Ultrason. Ferroelect. Freq. control*, vol. 58, no. 12, pp. 2699-2707, Dec. 2011.

[12] T. Kim, S. Shin, H. Lee, H. Kim, H. Shin, E. Kim, and S. Kim, "Matlab/Simulink pulse-echo ultrasound system simulator based on experimentally validated models," *IEEE Trans. Ultrason. Ferroelect. Freq. control*, vol. 63, no. 2, pp. 290-302, Feb. 2016.

[13] Fully Integrated, 8-Channel Ultrasound Analog Front End with Passive CW Mixer, 0.75 nV/rtHz, 14/12-Bit, 65 MSPS, 153 mW/CH, Texas Instruments Inc., 2014, Data Sheet AFE5808.

[14] 16-ch High Voltage Analog Switching IC, Hitachi Inc., Tokyo, Data Sheet ECN3297TF.

[15] Quad ±90 V, ±2A, 3/5 levels, High-speed Ultrasound Pulser, ST Microelectronics, 2012, Data Sheet STHV748.

[16] B. Gustavsen and A. Semlyen, "Rational approximation of frequency domain responses by vector fitting," *IEEE Trans. Power Del.*, vol. 14, no. 3, pp. 1052-1061, Jul. 1999.

[17] R. Zeng and J. Sinsky, "Modified rational function modeling technique for high speed circuits," in Proc. *IEEE MIT-S Int. Microw. Symp. Dig.*, San Francisco, USA, Jun. 11-16, 2006, pp. 1951-1954.

[18] L. Svilainis and V. Dumbrava, "Evaluation of the ultrasonic transducer electrical matching performance," *Ultrasound*, vol. 62, pp. 16-21, 2007.

**Sangmin Shin** received B.S. degree in electrical engineering and computer science from the University of California at Berkeley, Berkeley, CA, USA, in 2013. He is currently pursuing the Ph.D. degree in electrical and computer engineering from Seoul National University, Seoul, South Korea. His research interests include sensor interface circuits, analog front-end circuits, and analog-to-digital converters.

**Taehoon Kim** received the B.S., M.S., and Ph.D. degrees in electrical and computer engineering from Seoul National University, Seoul, Korea, in 2009, 2012 and 2017, respectively. From 2017 to 2018, he was with the Foundry Division, Samsung Electronics, Hwasung, Korea. Now, he joined the Delft University of Technology in the Netherlands, as a postdoctoral researcher. His main research interests are in the design of sensor interface circuits, beamformers, and analog-to-digital converters for ultrasound medical imaging application.

**Suhwan Kim** received the B.S. and M.S. degrees in electrical engineering and computer science from Korea University, Seoul, Korea, in 1990 and 1992, respectively, and the Ph.D. degree in electrical engineering and computer science from the

University of Michigan, Ann Arbor MI, in 2001. From 1993 to 1999, he was with LG Electronics, Seoul Korea. From 2001 to 2004, he was a Research Staff Member in IBM T. J. Watson Research Center, Yorktown Heights NY, USA. In 2004, he joined Seoul National University, Seoul, South Korea, where he is currently a Professor of Electrical and Computer Engineering. His research interests include analog and mixed-signal integrated circuits, high-speed I/O circuits, and silicon-photonic integrated circuits. Dr. Kim has received the 1991 Best Student Paper Award of the IEEE Korea Section and the First Prize (Operational Category) in the VLSI Design Contest of the 2001 ACM/IEEE Design Automation Conference, the Best Paper Award of the 2009 Korean conference on semiconductors, and the 2011 Best Paper Award of the International Symposium on Low-Power Electronics and Design. He served as a guest editor for the IEEE Journal of Solid-State Circuits special issue on the IEEE Asian Solid-State Circuits Conference. He has also served as the Organizing Committee Chair for IEEE Asian Solid State Conference and General Co-chair and Technical Program Chair for the IEEE International System-on-Chip (SoC) Conference. He has participated multiple times on the Technical Program Committee of the IEEE International SOC Conference, the International Symposium on Low-Power Electronics and Design, the IEEE Asian Solid-State Circuits Conference, and the IEEE International Solid-State Circuits Conference.